

# Chapter 3

## The Microscopic Description of a Macroscopic Experiment

Silvana Botti and Matteo Gatti

### 3.1 Introduction

The interaction between electromagnetic radiation (or particles) and matter creates elementary excitations in an electronic system. On one hand, this leads to phenomena (often complicated) that can be relevant in a variety of technological fields, including electronics, energy production, chemistry and biology. On the other hand, there is a fundamental interest in perturbing a material: the perturbation can indeed reveal essential material properties that were not detectable in the ground state of the system. To visualize this idea we can imagine a bell. In its ground state we cannot know what is the sound that it will produce when it is hit by a hammer. By perturbing the system, one can hear which is the characteristic frequency of the system, i.e. measure its elementary excitations.

According to the experimental setup, one can get access to different excitation properties. For example, in an experiment when an electron is added or removed, it is possible to gain insight into elementary one-particle excitations, i.e. the quasi-particles. When the number of electrons is conserved, the experiment will instead

---

S. Botti (✉)

Laboratoire des Solides Irradiés and ETSF,  
École Polytechnique, CNRS, CEA-DSM,  
91128 Palaiseau, France  
e-mail: silvana.botti@polytechnique.edu

and

LPMCN, Université Claude Bernard Lyon I and CNRS,  
69622 Villeurbanne, France

M. Gatti

Nano-Bio Spectroscopy Group and ETSF Scientific Development Centre,  
Departamento de Física de Materiales, Universidad del País Vasco,  
Centro de Física de Materiales CSIC-UPV/EHU-MPC and DIPIC,  
Avenida Tolosa 72, E-20018 San Sebastián, Spain  
e-mail: matteo.gatti@ehu.es

provide information on neutral excitations, such as excitons (electron-hole pairs) and plasmons (coherent electron oscillations). In a similar way, thanks to the powerful combination of state-of-the-art quantum-based theories and dedicated software in continuous development, it is now possible to study electronic excitations in complex materials. Within the many-body framework, to simulate a process involving one-particle excitations one deals with quantities related to the one-particle Green's function. In the case of neutral excitations the process can be described by response functions, a particular class of two-particle Green's functions.

A review of the different theoretical approaches and experimental techniques is beyond the aim of this chapter. We will focus on two specific aspects. First, one should keep in mind that while experiments usually measure macroscopic properties, *ab initio* calculations yield microscopic functions that need to be processed to obtain quantitative information comparable with measured spectra. In order to bridge the gap between the microscopic and the macroscopic worlds, one needs appropriate physical models that relate microscopic and macroscopic response functions. Second, depending on the details of the physical problem under study, one has to choose which theoretical approach and which level of approximation is more suitable for calculating the microscopic response functions. Moreover, one has to be aware of the fact that the accuracy and efficiency of calculations vary necessarily with the theoretical framework employed.

## 3.2 Theoretical Spectroscopy

We learned from [Chap. 2](#) that spectroscopies are ideal tools to investigate the electronic properties of extended and finite systems. What we commonly call “spectrum” is the response of a sample to a perturbation, which can be produced by an external electromagnetic field (photons) or by other particles (e.g. electrons, neutrons). This response is measured and plotted as a function of the frequency (or equivalently of the wavelength) of the incident particle.

By determining the energy (and possibly the wavevector and the spin) of the incoming and outgoing particles, it is possible to extract important information on the elementary excitations that were induced in the matter by the perturbation. Here, we restrict our interest to electronic properties, and more in particular to excitations involving valence electrons. The excitation energies will therefore be in the interval which goes from infra-red to ultraviolet radiation (up to some tens of eV), and which contains the visible portion of the electromagnetic spectrum. For such photon energies, the wavelength of the incoming radiation is always much larger than inter-atomic distances, which means that we can safely assume to be working in the long-wavelength limit. Moreover, we will consider only the first-order (linear) response, and we will not deal with strong-field interaction (e.g. intense lasers), nor with magnetic materials.

Existing spectroscopy techniques are numerous and can be classified according to different criteria. In [Table 3.1](#) we summarize the characteristics of a selected set

**Table 3.1** The spectroscopy techniques discussed in this chapter can be classified according to the probe used ('in'), the particle collected after the interaction with the sample ('out'), and the possible change in the number  $N$  of electrons in the sample

	In	Out	Number of $e^-$
Direct photoemission	photon	electron	$N \rightarrow N - 1$
Inverse photoemission	electron	photon	$N \rightarrow N + 1$
Photoabsorption	photon	photon	$N \rightarrow N$
Electron energy loss	electron	electron	$N \rightarrow N$

of processes. They are classified according to the probe used (electromagnetic field, electron, etc.), what is collected and measured after the interaction with the electronic system (again, electromagnetic field, electron, etc.), and whether the number of electrons in the system remains fixed, or if electrons are added or removed. The following sections are devoted to an introduction to the phenomenology of these spectroscopies, in order to specify which are the physical quantities that are measured, and that we therefore want to calculate.

In Sect. 3.3 we give examples of experiments involving one-electron excitations, i.e. in which an electron is added or removed from the system. In a photoemission (PES) process the system of interacting electrons absorbs one photon with enough energy to excite an electron (called photoelectron) above the vacuum level. The missing electron leaves a hole in the system, which generally remains in an excited state. The kinetic energy distribution of the photoelectron can be measured by the analyser, yielding the photoemission spectrum. In the simple independent-particle picture, photoemission spectra give an image of the density of the occupied electronic states of the sample. Inverse photoemission can be considered as the time-reversal process of photoemission: in this case the system absorbs an electron and a photon is emitted, whose energy distribution can be related in the independent-particle picture to the density of empty states. However, one should not forget that the sample is a many-body system. In the many-body framework, one has rather to deal with one-particle Green's functions and spectral functions, in order to extract from them physical quantities to compare with photoemission spectra.

In Sect. 3.4 we discuss two examples of processes involving neutral excitations: optical absorption and electron energy loss. In an absorption experiment the incident beam of light loses photons that are absorbed by the system. Their energy is used to excite an electron from an occupied to an empty state: an electron-hole pair is then created in the system. Instead, in electron energy-loss spectroscopy (EELS) experiments an electron undergoes an inelastic scattering with the sample. The analyser measures its energy loss and its deflection. Again, the energy lost by the incoming electron has been used to induce excitations in the system. Response functions, a particular class of two-particle Green's functions, are the key quantities to explore neutral excitations and will be presented in Sect. 3.5. From the theoretical point of view, the frequency and wavevector dependent dielectric functions  $\epsilon(\mathbf{q}, \omega)$  and its inverse  $\epsilon^{-1}(\mathbf{q}, \omega)$  are the most natural quantities for the description of the neutral

excitations of an extended system. In a non-isotropic medium such functions must be replaced by tensors. Moreover, it should be emphasised that a electromagnetic field is a transverse field (i.e. the field is perpendicular to the direction of propagation), while impinging electrons are associated to longitudinal fields (i.e. their field is along the direction of propagation). This implies the existence of transverse (T) and longitudinal (L) dielectric functions. In [Sect. 3.6](#) we will finally show how dielectric functions, inserted in appropriate semi-classical models, and through appropriate averaging procedures, yield the frequency-dependent spectra to be compared with experimental data. Atomic units will be used throughout the chapter.

### 3.3 Photoemission Spectra and Spectral Functions

At the heart of photoemission spectroscopy lays the photoelectric effect. Discovered by Hertz in 1887, its experimental study was worth a Nobel prize for Lenard and its theoretical explanation another Nobel prize for Einstein. An example of experimental valence photoemission spectrum, taken from Guzzo et al. (2011), is displayed in [Fig. 3.1](#). In this section we will discuss how to calculate a quantity directly comparable with such a spectrum starting from first principles. For a more general description of photoemission spectroscopy we refer to [Chap. 2](#) and to the many books and reviews available in literature [e.g. (Hüfner 2003; Schattke and Van Hove 2003; Damascelli et al. 2003; Almladh and Hedin 1983)].

The simplest phenomenological interpretation of the photoemission process is given by the so-called three-step model (Berglund and Spicer 1964), which describes photoemission as a sequence of the actual excitation process, the transport of the photoelectron to the crystal surface, and the escape into the vacuum. A better interpretation is obtained in the one-step model (Schaich and Ashcroft 1970; Mahan 1970; Pendry 1976), where the three different steps are combined in a single coherent process, described in terms of direct optical transitions between many-body wavefunctions that obey appropriate boundary conditions at the surface of the solid. The final state of the photoelectron is a time-reversed low-energy electron-diffraction (LEED) state, which has a component consisting of a propagating plane-wave in vacuum with a finite amplitude inside the crystal.

The measured data are the energy of the incoming photon and the kinetic energy of the outgoing electron. In an angular-resolved experiment (ARPES) also the angle of emission is detected, which allows the evaluation of the wavevector of the emitted photoelectron. Moreover, using a Mott detector it is also possible to perform a spin analysis.

When an electron is removed from an electronic system, the measured photocurrent  $J_k(\omega)$  is given by the probability per unit time of emitting an electron with momentum  $\mathbf{k}$  when the sample is irradiated with photons of frequency  $\omega$ . From Fermi's golden rule one obtains the relation (Almladh and Hedin 1983; Hedin 1999):

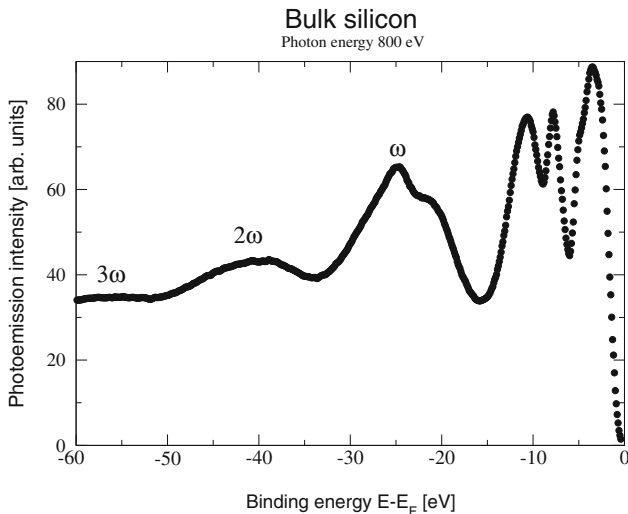


**Fig. 3.1** Experimental photoemission spectrum of bulk silicon, measured at the TEMPO beamline at the Synchrotron SOLEIL with 800 eV photon energy. Besides the prominent quasiparticle peaks, corresponding to the valence bands, multiple plasmon satellites at higher binding energies are clearly visible. Figure from Guzzo (2011)

$$J_{\mathbf{k}}(\omega) = \sum_m \xi_{km} \delta(E_{\mathbf{k}} - E_m - \omega), \quad (3.1)$$

where

$$\xi_{km} = |\langle N-1, m; \mathbf{k} | \mathbf{A} \cdot \mathbf{p} + \mathbf{p} \cdot \mathbf{A} | N \rangle|^2 \quad (3.2)$$

is a matrix element of the coupling to the photon field and  $|N\rangle$ ,  $|N-1, m; \mathbf{k}\rangle$  are many-body states. The perturbation induces a transition from the initial  $N$ -electron ground state  $|N\rangle$  to the final state  $|N-1, m; \mathbf{k}\rangle$ . The final state is represented by a system with the photoelectron with momentum  $\mathbf{k}$  and the sample in the excited state  $m$  with  $N-1$  electrons. In order to assure the energy conservation, it is required that the photon energy  $\omega$  is equal to the kinetic energy of the photoelectron  $E_{\mathbf{k}}$  minus the electron removal energy,  $E_m = E(N) - E(N-1, m)$ . This reads  $\omega = E_{\mathbf{k}} - E_m$ . By knowing  $\omega$  and measuring  $E_{\mathbf{k}}$ , one can have access to the energy of the excited state  $m$ .

In the sudden approximation, the photoelectron is completely decoupled from the sample. One assumes that the photoelectron does not interact with the hole left behind and does not affect the state of the  $(N-1)$  electron system. Under such hypothesis, the total photocurrent  $J_{\mathbf{k}}(\omega)$  can be rewritten as:

$$J_{\mathbf{k}}(\omega) = \sum_i |\xi_{ki}|^2 A_{ii}(E_{\mathbf{k}} - \omega), \quad (3.3)$$

where we have introduced the matrix elements of the spectral function  $A_{ij}(\omega)$  (for  $\omega$  below the Fermi level) and the creation and annihilation operators  $\hat{c}^\dagger$  and  $\hat{c}$ :

$$A_{ij}(\omega) = \sum_m \left\langle N \left| \hat{c}_i^\dagger \right| N-1, m \right\rangle \langle N-1, m | \hat{c}_j | N \rangle \delta(\omega - E_m), \quad (3.4)$$

and, moreover, we have assumed that there exists a one-particle basis in which the diagonal elements of  $A_{ij}$  are the relevant terms. For each many-body state  $m$ , the spectral function (3.4), defined rigorously as the imaginary part of the one-particle Green's function  $G$ , gives the probability to remove an electron from the ground state  $|N\rangle$  and leave the system in the excited state  $|N-1, m\rangle$ . The total intensity of the photoemission spectrum is then the sum of the diagonal terms of spectral function  $A_{ii}$ , weighted by the photoemission matrix elements  $\xi_{ki}$ . Therefore, when the matrix elements are not zero, photoemission measurements give direct insight into the spectral function  $A$ .

The matrix elements  $\xi_{ki}$  describe the dependence of the spectra on the energy, momentum and polarization of the incoming photon. However, a common approximation is to neglect those matrix elements or, equivalently, to assume they are all equal to a constant  $\bar{\xi}$ , which yields:

$$J_k(\omega) = |\bar{\xi}|^2 \sum_i A_{ii}(E_k - \omega). \quad (3.5)$$

Hence, to a first approximation, the quantity that one needs to calculate to simulate photoemission spectra is the trace of the spectral function (Gatti et al. 2007a).

In a simplified independent-particle picture, by measuring the kinetic energy of the emitted electron, one would obtain directly the energy of the one-particle level that the electron was occupying before being extracted from the sample. In this picture the many-body wavefunctions are Slater determinants and the spectral function (3.4) can be simplified to yield

$$A_{ij}(\omega) = \delta_{ij} \delta(\omega - E_i) \theta(\mu - \omega). \quad (3.6)$$

The total photocurrent

$$J_k(\omega) = |\bar{\xi}|^2 \sum_i^{occ} \delta(E_k - \omega - E_i) \quad (3.7)$$

turns out to be given by a series of delta peaks in correspondence to the energies  $E_i$  of the one-particle Hamiltonian. The photoemission spectrum is hence described by the density of occupied states:

$$\text{DOS}(E_k - \omega) = \sum_i^{occ} \delta(E_k - \omega - E_i), \quad (3.8)$$

evaluated at the energy  $E_k - \omega$ .

However, the real system is made of interacting electrons, and the distribution of kinetic energies that one actually obtains is somewhat different from this ideal picture. In fact, it is easy to understand that the emitted electron leaves a hole in the electronic system. A hole is a depletion of negative charge, hence it carries a positive charge which induces a relaxation of all the other electrons in order to screen it. Therefore, the creation of a hole promotes an excited state in the system, with a finite lifetime. This explains why in a photoemission spectrum one does not find a delta-peak in correspondence to a particular one-particle binding energy.

If one wants to perform calculations beyond the independent-particle picture, the many-body wavefunctions can then be seen as linear combinations of Slater determinants. For each excited state  $m$ , there are many non-vanishing contributions to the spectral function (3.4) that give rise to a more complex structure around the energy  $E_m$ . If in this more complex structure a main peak is still identifiable, then one can associate this peak with a quasiparticle excitation.

More complex phenomena can actually happen when the electron is extracted from the sample. In fact, the hole left in the system is itself a perturbation that can induce additional excitations. For example, a plasmon can be additionally excited in the system. In this case, the incoming photon energy is used to create more than one excitation. This additional excitations will produce a peak in the photoemission spectrum at a higher binding energy and with a smaller intensity than the corresponding quasiparticle peak, which reflects the smaller probability of a combination of events and its larger energy cost. This kind of additional structures in a photoemission spectrum is called a satellite and forms the incoherent part of the spectrum.

A clear example is given by the experimental spectrum of bulk silicon in Fig. 3.1. The three prominent peaks at lower binding energy are the quasiparticle peaks that correspond to the valence bands of silicon. Together with these peaks, we can see three additional structures with decreasing intensities, located at distances from the quasiparticle peaks equal to multiples of the plasmon energy of bulk silicon (around 16 eV). They are plasmon replicas: satellites that are the signature of the additional simultaneous excitation of one, two and three plasmons, respectively. This is a striking example that shows that photoemission spectroscopy is able to measure not only one-particle-like excitations (the quasiparticles), but also collective excitations, like plasmons (which can be directly measured in electron energy-loss spectroscopy, see Sect. 3.4).

In the extreme case of strong-correlation effects in the system, the one-particle nature of the excitation can be completely lost. In this case, in fact, it is no more possible to distinguish quasiparticle peaks, as all excitations involved have an intrinsic many-body character and the incoherent part of the spectrum dominates.

A spectral function for the metallic phase of VO<sub>2</sub>, calculated in the *GW* approximation (Hedin 1965), is shown in Fig. 3.2. In order to gain a deeper insight into the nature of the structures of the spectral function, we can rewrite its matrix elements (3.4) in terms of the self-energy  $\Sigma$  (Hedin 1999):

$$A_{ii}(\omega) = \frac{1}{\pi} \frac{|\Im \Sigma_{ii}(\omega)|}{\{\omega - \varepsilon_i - [\Re \Sigma_{ii}(\omega) - v_{xci}]\}^2 + [\Im \Sigma_{ii}(\omega)]^2}, \quad (3.9)$$

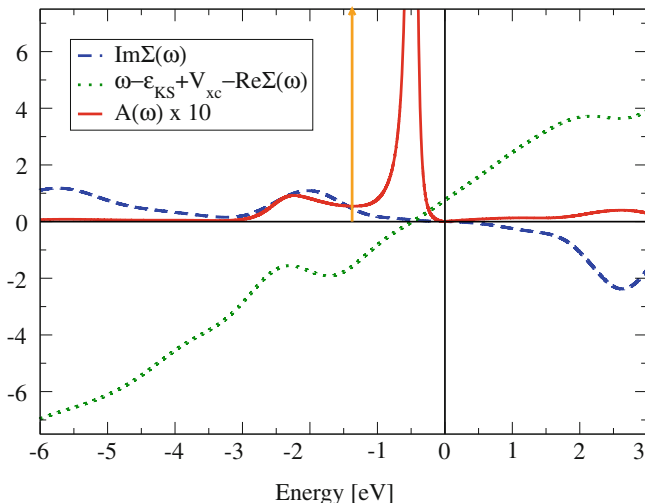


**Fig. 3.2** Spectral function  $A_{ii}$  (red solid line) relative to the top valence at  $\mathbf{k} = \Gamma$  for the metallic phase of  $\text{VO}_2$ , calculated using the  $GW$  approximation. The corresponding Kohn–Sham eigenvalue, calculated in the local-density approximation, is represented by the arrow. The real and imaginary parts of the self-energy  $\Sigma$  are also shown (see the discussion in the text). The zero of the energy axis is set at the  $GW$  Fermi energy.

where we have assumed that the self-energy is diagonal in the one-particle basis chosen to represent the spectral function  $V_{xci}$  are the matrix elements of the  $x$ c potential and  $\varepsilon_i$  are the Kohn–Sham eigenvalues. The self-energy is an essential quantity in the Green’s function formalism. It represents, in fact, the effective non-local and dynamical potential that the extra particle feels for the polarization that its propagation induces and for the exchange effects, due to the fact that it is a fermion. Analogously to the exchange–correlation potential  $v_{xc}$  of density-functional theory (DFT), the self-energy encompasses all the effects of exchange and correlation in the system.

Equation 3.9 allows us to see that the quasiparticle peak in the spectral function shown in Fig. 3.2 is determined by the zero of  $\omega - \varepsilon_i - [\Re \Sigma_{ii}(\omega) - v_{xci}]$ . The width of the peak is given by the imaginary part of the self-energy: the quasiparticle excitation has finite lifetime (which is the inverse of the width of the peak). Additional structures, the satellites, are linked to structures of  $\Im \Sigma_{ii}(\omega)$  or to additional zeros of  $\omega - \varepsilon_i - [\Re \Sigma_{ii}(\omega) - v_{xci}]$ , where also  $\Im \Sigma_{ii}(\omega)$  is not too large. Note that a necessary requirement for the presence of satellites is the dynamical nature of  $\Sigma$ . In particular, in the case of  $\text{VO}_2$  shown in Fig. 3.2, we can see a satellite in the spectral function due to a structure of  $\Im \Sigma_{ii}(\omega)$ , which corresponds to the additional excitation of a plasmon (Gatti 2007b). This situation is analogous to what we have discussed for the experimental spectrum of silicon in Fig. 3.1. In a Kohn–Sham calculation within DFT, the spectral function would reduce to a delta peak, represented by the arrow in Fig. 3.2. The same would occur in the Hartree–Fock



approximation, in which the self-energy is real and static. In Hartree–Fock, thanks to Koopmans’ theorem (Koopmans 1934), the eigenvalues have a physical meaning as approximate removal energies, contrary to the Kohn–Sham eigenvalues, for which Koopmans’ theorem does not hold.

When one goes beyond the sudden approximation (Hedin 1998; Almbladh 2006) and considers scattering processes of the photoelectron on its way out of the sample, new features in the photoemission spectrum can appear. In this case one talks of extrinsic losses, in contrast to the structures of the spectral function discussed so far, and that are due to intrinsic losses.

Moreover, in order to restore a quantitative agreement between calculated and measured spectra, one should keep in mind that it is essential to remove the assumption that the photoemission matrix elements  $\xi_{ki}$  are constant. In fact, measured spectra generally show large variations in their profile according to the photon energy used in the experiment (Papalazarou 2009).

Since the electron escape depth is of the order of 10–50 Å for kinetic energies of 10–2000 eV (Zangwill 1988), photoemission is a surface sensitive technique. Obtaining bulk information can be achieved by using atomically flat and clean surfaces and by working at high photon energies [e.g. hard X-rays (Panaccione 2006)], thereby increasing the electron escape depth. At the same time, higher photon energies are in better agreement with the hypothesis of the sudden approximation, as the photoelectron is emitted with a high kinetic energy, and therefore its removal process can be more safely considered as instantaneous. Nevertheless, angular-resolved experiments are performed at lower photon energies, where the intrinsic momentum resolution is better (Damascelli 2003).

### 3.4 Microscopic Description of Neutral Excitations

The propagation of electromagnetic waves in dissipative media is described by Maxwell’s equations (Jackson 1962), supplemented by appropriate constitutive equations. Optical phenomena (reflection, propagation, transmission) can be quantified by a number of parameters that determine the properties of the medium at the macroscopic level. Microscopic (semiclassical) models and averaging procedures then allow us to calculate these macroscopic parameters. In this section we focus on the microscopic models, while the averaging procedure will be the subject of [Sect. 3.6](#).

A photon impinging on a sample can be absorbed, reflected or transmitted. When it is absorbed, its energy is used to create a neutral excitation in the system. In an independent-particle picture, this can be represented by the promotion of a valence electron from an occupied to an empty one-particle state, conserving its crystal momentum  $\mathbf{k}$ , since a photon in the energy range of interest can transfer only a negligible momentum. In contrast with what happens in a photoemission experiment, the excited electron remains inside the sample, and it cannot therefore be considered decoupled from the other electrons.

According to the semi-classical picture provided by the macroscopic Maxwell equations (Jackson 1962), an electric field  $\mathbf{E}$  polarized along the  $\hat{\mathbf{e}}$  direction in a dielectric medium propagates as a damped wave:

$$\mathbf{E}(z, t) = E_0 \hat{\mathbf{e}} e^{i\frac{\omega}{c}(nz-ct)} = E_0 \hat{\mathbf{e}} e^{i\frac{\omega}{c}(n_1 z - ct)} e^{-\frac{\omega}{c} n_2 z}, \quad (3.10)$$

where  $n$  is the complex refractive index  $n = n_1 + in_2$ , and  $c$  is the velocity of light in vacuum. As a consequence, also the intensity of the field is exponentially decaying:

$$I(z) = |\mathbf{E}(z)|^2 = E_0^2 e^{-2\frac{\omega}{c} n_2 z}. \quad (3.11)$$

The absorption coefficient  $\alpha^{\text{abs}}$  is defined as the inverse of the distance where the intensity of the field is reduced by  $1/e$ :

$$\alpha^{\text{abs}} = \frac{2\omega n_2}{c}. \quad (3.12)$$

Equivalently, we can introduce the concept of macroscopic complex dielectric function  $\epsilon_M = \epsilon_1 + i\epsilon_2 = n^2$ .

The absorption coefficient can be easily rewritten in terms of the imaginary part of the macroscopic dielectric function:

$$\alpha^{\text{abs}} = \frac{\omega \epsilon_2}{c n_1}. \quad (3.13)$$

Since  $n_1$  can be usually assumed constant in the small frequency ranges of interest, absorption spectra are usually expressed in terms of  $\epsilon_2(\omega) = \mathcal{I}m \epsilon_M(\omega)$ .

Within the basic approximations, i.e. the independent-particle and the dipole approximation, Fermi's golden rule (Grosso 2000) gives the well-known expression for the absorption spectrum in the linear regime, as a sum of one-particle independent transitions:

$$\epsilon_2^{\text{TT}}(\omega) = \frac{8\pi^2}{\mathcal{V}\omega^2} \sum_{vc} |\langle \varphi_c | \hat{\mathbf{e}} \cdot \mathbf{p} | \varphi_v \rangle|^2 \delta(E_j - E_i - \omega), \quad (3.14)$$

where  $\mathbf{p}$  is the momentum operator,  $\mathcal{V}$  is the unit cell volume,  $|\varphi_{v,c}\rangle$  are one-particle states (e.g. Kohn–Sham states) and  $E_i$  are one-particle energies (e.g. Kohn–Sham energies). In (3.14) T stands for transverse, as the transitions from occupied to empty states  $|\varphi_c\rangle$  to  $|\varphi_v\rangle$  are due to the interaction with a transverse electromagnetic plane wave of frequency  $\omega$  and polarization  $\hat{\mathbf{e}}$ . In general one should consider different polarization directions, which means that  $\hat{\epsilon}_2$  is a tensor. This tensor reduces to a scalar quantity when the system is isotropic (cubic symmetry).

Note that in the simple case of a sum of independent one-particle transitions the macroscopic dielectric function is simply the spatial average of the microscopic dielectric function  $\epsilon(\mathbf{r}, \mathbf{r}', t - t')$ . This means that classical depolarization effects (local-field effects) are not included in Eq. 3.14. We will go back to this problem, related to spatial averaging, in the following section.

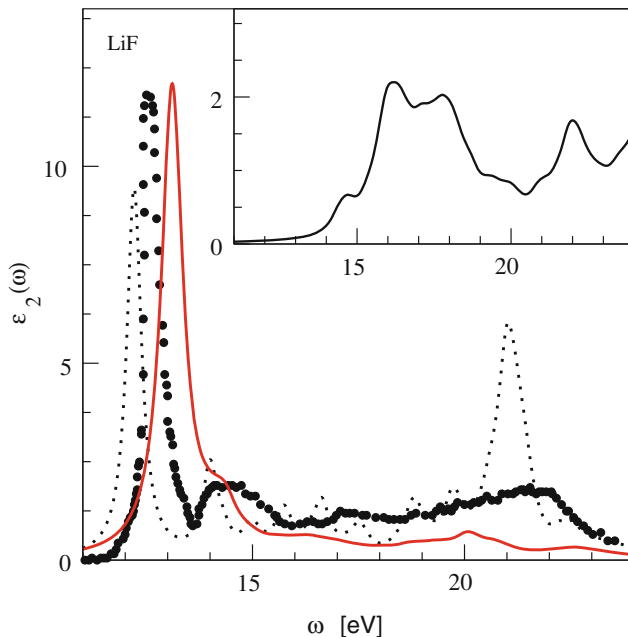


**Fig. 3.3** Imaginary part of the macroscopic dielectric function for LiF. *Dots*, experiment from (Roessel 2005); *dotted line*, Bethe-Salpeter equation (BSE) calculation; *solid line*, TDDFT calculation using the dynamical model kernel derived from BSE. In the *inset*, RPA calculation using quasiparticle energies. Figure from Botti (2005)

Local-field effects are not the only missing physical ingredient. In fact, the independent-transition picture is often inadequate to capture the complex physics of the many-body problem and, even if local-field effects are properly accounted for, the quality of the calculated spectra still depends dramatically on the use of more involved approximations to include electron-electron and electron-hole interactions. Indeed, one should not forget that in an absorption experiment, contrary to photoemission, the excited electron remains inside the system. It is essential then to take into account the interaction between the electron and the hole that the excitation of the electron leaves behind, the so-called excitonic effect. This can be done in different frameworks that go beyond the independent-particle approximation, such as many-body perturbation theory, or time-dependent density-functional theory.

We consider as an example a LiF crystal (Botti 2005), whose experimental absorption spectrum (dots) is shown in Fig. 3.3. If one performs a calculation in the independent-particle approximation, even after including local-field effects within the random phase approximation (RPA) (inset), the worst disagreement concerns the absence of the large excitonic peak at about 12.5 eV. In the framework of many-body perturbation theory, it is possible to include two-quasiparticle effects by solving the Bethe-Salpeter equation (BSE) (Salpeter 1951). In this way, one can reproduce the

bound exciton peak (dotted-dashed curve). Alternatively, one can use, within time-dependent density functional theory (TDDFT), model exchange-correlation kernels derived from the Bethe-Salpeter equation (Botti 2007), which improve remarkably the RPA results with a much smaller computational effort than the one required by the solution of the Bethe-Salpeter equation.

Another example of neutral excitations comes from electron energy-loss spectroscopy, where the probe is a high-energy electron which undergoes inelastic scattering. As a consequence, it loses energy and has its path deflected. Both the energy loss and the deflection angle can be measured. Inelastic interactions can involve different energy ranges, depending on their origin: phonon excitations, inter- or intra-band transitions, plasmon excitations, inner-shell ionizations, Auger processes, etc. In the energy range that we consider (up to some tens of eV), the excitations of the system that can be involved are either band transitions or plasmon excitations.

We consider the rate by which a charged fast particle transfers energy and momentum to a material. As long as the fractional changes of energy and momentum of the fast electron are small, the electron can be considered as a classical point charge moving with uniform velocity  $\mathbf{v}$  in the medium. The probability that an impinging electron of velocity  $\mathbf{v}$  transfers in a unit time an energy  $dW$  and a momentum  $\mathbf{q}$  to the electronic system can be expressed by the energy-loss rate (Luth 2001):

$$\frac{dW}{dt} = \frac{1}{(2\pi)^3} \int d\omega \int d^3q \frac{\omega}{q^2} \Im m \left\{ -\frac{1}{\epsilon_M(\mathbf{q}, \omega)} \right\} \delta(\omega + \mathbf{q} \cdot \mathbf{v}). \quad (3.15)$$

In (3.15) one assumes that the impinging electron is a classical particle: it can be treated in a non-relativistic approximation and neglecting quantum indetermination effects on its position. The energy-loss rate is then proportional to the loss function  $L(\mathbf{q}, \omega)$ :

$$L(\mathbf{q}, \omega) = -\Im m \left\{ \frac{1}{\epsilon_M(\mathbf{q}, \omega)} \right\} = \frac{\epsilon_2(\mathbf{q}, \omega)}{\epsilon_1^2(\mathbf{q}, \omega) + \epsilon_2^2(\mathbf{q}, \omega)}. \quad (3.16)$$

From Eq. 3.16 one can conclude that spectral features in EELS can be seen in the case that either  $\epsilon_2$  has a peak corresponding to some interband transition or  $\epsilon_2$  is small and  $\epsilon_1 = 0$ . The latter condition determines the frequencies of the collective plasmon excitations. In energy-loss experiments one can therefore excite plasmons, that are longitudinal excitations and that are not generally observed in optical spectroscopy, since photons are a transverse perturbation. Note that the loss function (3.16) is also the quantity measured in inelastic X-rays scattering (IXS) experiments.

An interesting situation can be found in the study of EELS for core states. In fact, at high energies  $\epsilon_2(\mathbf{q}, \omega) \rightarrow 0$  and  $\epsilon_1(\mathbf{q}, \omega) \rightarrow 1$ . This observation allows a simplification of the loss function (3.16):

$$L(\mathbf{q}, \omega) = -\Im m \left\{ \frac{1}{\epsilon_M(\mathbf{q}, \omega)} \right\} \rightarrow \epsilon_2(\mathbf{q}, \omega). \quad (3.17)$$

Using again the simple independent one-particle transition picture, Fermi's golden rule allows us to evaluate the imaginary part of the longitudinal dielectric function as Grosso (2000):

$$\epsilon_2^{\text{LL}}(\mathbf{q}, \omega) = \frac{8\pi^2}{\mathcal{V}q^2} \sum_{ij} \left| \langle \varphi_j | e^{i\mathbf{q}\cdot\mathbf{r}} | \varphi_i \rangle \right|^2 \delta(E_j - E_i - \omega), \quad (3.18)$$

where LL means that we are evaluating the response to a longitudinal perturbation. In this picture plasmon peaks in EELS are associated to coherent oscillations of independent particles. Once again, the quality of the calculated spectra depends dramatically on the possibility to go beyond the independent-particle description of Eq. 3.18. For extended systems, EELS and IXS at small and large momentum transfer are often well reproduced simply by including local-field effects, i.e. performing RPA calculations or TDDFT calculations within the adiabatic local-density approximation (TDLDA—Botti 2007). This is in contrast with the fact that TDLDA fails in the calculation of optical ( $\mathbf{q} = 0$ ) spectra of non-metallic solids. To explain this failure, the wrong asymptotic limit of the exchange-correlation kernel is crucial, while the wrong behaviour of the exchange-correlation potential is less relevant (Botti 2007).

Note again that we defined two different microscopic dielectric functions,  $\epsilon_2^{\text{LL}}$  and  $\epsilon_2^{\text{TT}}$ , specific for longitudinal and transverse perturbations, respectively. However, since it holds (Del Sole 1993):

$$\mathbf{v} = \lim_{q \rightarrow 0} \frac{1}{q} \left[ \hat{H}, e^{i\mathbf{q}\cdot\mathbf{r}} \right], \quad (3.19)$$

it can be proved that in the long-wavelength limit longitudinal (3.18) and transverse (3.14) dielectric functions of an isotropic system coincide:

$$\epsilon_{\text{M}}^{\text{LL}}(\omega) = \epsilon_{\text{M}}^{\text{TT}}(\omega). \quad (3.20)$$

This is due to the invariance for  $\mathbf{q} \rightarrow 0$  between the velocity gauge (transverse perturbation  $\mathbf{A} \cdot \mathbf{v}$ ) and the length gauge (longitudinal perturbation  $\mathbf{E} \cdot \mathbf{r}$ ). When  $\mathbf{q}$  is non-vanishing and the system does not have cubic symmetry, this extreme simplification is no more valid, and one has to consider the general tensor.

### 3.5 Microscopic Response Beyond the Independent-Particle Picture

We will now deal with the general problem of the determination of the microscopic response of the system, beyond an independent-particle picture and Fermi's golden rules 3.14 and 3.18. In the following section we will then discuss how to relate microscopic and macroscopic dielectric functions. Linear-response theory can be applied to study the response of an electronic system to a small time-dependent

perturbation  $\hat{V}_{\text{ext}}(t)$ , such as the incoming electromagnetic field or the high-energy electron which undergoes inelastic scattering that we discussed before. We consider here a system described by the many-body Hamiltonian  $\hat{H}$ , subjected to a time-dependent external perturbation  $\hat{V}_{\text{ext}}(t)$ . The total Hamiltonian becomes:

$$\hat{H}_{\text{tot}} = \hat{H} + \hat{V}_{\text{ext}}(t). \quad (3.21)$$

For a sufficiently small perturbation, the response of the system can be expanded into a Taylor series with respect to the perturbation. The linear coefficient linking the response to the perturbation is the response function. In this context, the density-density response function  $\chi$  is defined as

$$\delta\rho(\mathbf{r}, t) = \int dt' \int d^3r' \chi(\mathbf{r}, \mathbf{r}', t - t') v_{\text{ext}}(\mathbf{r}', t'), \quad (3.22)$$

where  $\delta\rho$  is the first-order variation of the electron density and  $v_{\text{ext}}$  the external perturbation. A response function is independent on the perturbation and depends only on the system. The density-density response function is also called reducible polarizability. The irreducible polarizability  $P$  can be defined in a similar way:

$$\delta\rho(\mathbf{r}, t) = \int dt' \int d^3r' P(\mathbf{r}, \mathbf{r}', t - t') v_{\text{tot}}(\mathbf{r}', t'), \quad (3.23)$$

where  $v_{\text{tot}}$  is the total classical potential. Hence, the irreducible polarizability  $P$  describes the first-order variation of the electron density with respect to the total classical potential, which includes the polarization of the system.

In fact, as a consequence of the polarization of the system due to the applied perturbation, the total potential becomes a sum of the external potential and the induced potential:  $v_{\text{tot}}(\mathbf{r}, t) = v_{\text{ext}}(\mathbf{r}, t) + v_{\text{ind}}(\mathbf{r}, t)$ . The induced potential  $v_{\text{ind}}$  and the induced density  $\delta\rho$  are moreover related by  $v_{\text{ind}} = v_{\text{ee}}\delta\rho$  ( $v_{\text{ee}}$  is the Coulomb interaction). The basic quantity that gives information about the screening of the system in linear response is the microscopic dielectric function, which relates the total potential to the applied potential:

$$v_{\text{tot}}(\mathbf{r}, t) = \int dt' \int d^3r' \epsilon^{-1}(\mathbf{r}, \mathbf{r}', t - t') v_{\text{ext}}(\mathbf{r}', t'). \quad (3.24)$$

Remembering the definition of the density-density response function  $\chi$  (3.22) we can easily deduce that the microscopic dielectric function  $\epsilon$  and  $\chi$  are related by

$$\epsilon^{-1}(\mathbf{r}, \mathbf{r}', t - t') = \delta(\mathbf{r} - \mathbf{r}')\delta(t - t') + \int d^3r'' v_{\text{ee}}(\mathbf{r} - \mathbf{r}'')\chi(\mathbf{r}', \mathbf{r}'', t - t'). \quad (3.25)$$

The microscopic dielectric function can also be related to the irreducible polarizability:

$$\epsilon(\mathbf{r}, \mathbf{r}', t - t') = \delta(\mathbf{r} - \mathbf{r}')\delta(t - t') - \int d^3r'' v_{\text{ee}}(\mathbf{r} - \mathbf{r}'')P(\mathbf{r}'', \mathbf{r}', t - t'). \quad (3.26)$$

Moreover, the reducible and irreducible polarizabilities satisfy the Dyson equation

$$\begin{aligned} \chi(\mathbf{r}, \mathbf{r}', t - t') &= P(\mathbf{r}, \mathbf{r}', t - t') + \int d^3 r'' \int d^3 r''' P(\mathbf{r}, \mathbf{r}'', t - t') v_{ee} \\ &\times (\mathbf{r}'' - \mathbf{r}''') \chi(\mathbf{r}''', \mathbf{r}', t - t'). \end{aligned} \quad (3.27)$$

The dielectric function is a quantity that is usually used to define the response of an extended system. Similar quantities and formulas can, however, be obtained also for finite systems. In the linear-response regime and dipole approximation, and considering that in the range of frequencies of interest (optical frequencies) the dimension of the system is much smaller than the radiation wavelength, the induced density variation in the finite system is again proportional to the perturbing field as defined by Eq. 3.22. For a dipole electric field along the direction  $z$ , the photoabsorption cross section along  $z$ ,  $\sigma_{zz}$ , is

$$\sigma_{zz}(\omega) = -\frac{4\pi\omega}{c} \Im m \left\{ \int d^3 r \int d^3 r' z \chi(\mathbf{r}, \mathbf{r}', \omega) z' \right\} = \frac{4\pi\omega}{c} \Im m \{ \alpha_{zz}(\omega) \}, \quad (3.28)$$

the above expression also serving as the definition of the dynamical polarizability  $\hat{\alpha}$ . Like  $\epsilon$ , the dynamical polarizability is in general a tensor and the photoabsorption cross section  $\sigma$  can be written in the form:

$$\sigma(\omega) = \frac{4\pi\omega}{3c} \Im m \{ \text{Tr} \hat{\alpha}(\omega) \}. \quad (3.29)$$

Another quantity that is often used for finite systems is the dipole strength function  $S$ :  $\sigma(\omega) = (2\pi^2/c)S(\omega)$ .

In linear-response theory, in general, we deal with perturbations that couple a time-dependent field  $F(t)$  to an observable of the system  $\hat{P}$ :

$$\hat{V}_{\text{ext}}(t) = \int d^3 r_1 F(\mathbf{r}_1, t) \hat{P}(\mathbf{r}_1, t). \quad (3.30)$$

Typically the perturbation is an electromagnetic field coupled with densities or currents. In linear-response one assumes that variations  $\delta F$  of the field  $F$  are small. From Kubo's formula (Kubo 1957) the variation  $\delta \langle \hat{O}(\mathbf{r}_1, t) \rangle$  of an observable  $\hat{O}$  is then obtained by using first-order perturbation theory as:

$$\delta \langle \hat{O}(\mathbf{r}_1, t) \rangle = \int dt' \int d^3 r_2 \chi_{\text{OP}}(\mathbf{r}_1, \mathbf{r}_2, t - t') \delta F(\mathbf{r}_2, t'), \quad (3.31)$$

where

$$\begin{aligned} \chi_{\text{OP}}(\mathbf{r}_1, \mathbf{r}_2, t - t') &= -i\theta(t - t') \langle N | [\hat{O}(\mathbf{r}_1, t), \hat{P}(\mathbf{r}_2, t')] | N \rangle \\ &= \frac{\delta \langle \hat{O}(\mathbf{r}_1, t) \rangle}{\delta F(\mathbf{r}_2, t')} \end{aligned} \quad (3.32)$$

is a (causal or retarded) response function and  $|N\rangle$  is the many-body ground-state wavefunction. In fact,  $\chi_{\text{OP}}$  is zero for  $t < t'$ , because there cannot be any response at a time  $t$  before a perturbation has occurred at a time  $t'$ .

By inserting the completeness relation and taking the Fourier transform, the response function can be written in the so-called Lehmann representation:

$$\chi_{\text{OP}}(\mathbf{r}_1, \mathbf{r}_2, \omega) = \lim_{\eta \rightarrow 0^+} \sum_m \left[ \frac{O_m(\mathbf{r}_1) P_m^*(\mathbf{r}_2)}{\omega + E_0 - E_m + i\eta} - \frac{O_m^*(\mathbf{r}_1) P_m(\mathbf{r}_2)}{\omega + E_m - E_0 + i\eta} \right], \quad (3.33)$$

where

$$O_m(\mathbf{r}_1) = \langle N | \hat{O}(\mathbf{r}_1) | N, m \rangle, \quad (3.34)$$

( $P_m$  is analogously defined) and  $\eta$  is a positive infinitesimal. The response function has poles at the excitation energies  $\pm(E_0 - E_m)$ , corresponding to transitions between the ground state  $|N\rangle$  and the many-body excited state  $|N, m\rangle$  of the unperturbed Hamiltonian  $\hat{H}$ . The first term in (3.22) is given by resonant transitions, the second by antiresonant transitions. The form of (3.22) is valid for finite systems with discrete eigenvalues. For extended systems, on the other hand, the spectrum is continuous, and the sum in (3.22) turns into an integral that gives rise to a branch cut along the real energy axis. The infinitely close-lying resonances thus merge into broad structures that can be identified with elementary excitations, such as plasmons or excitons. As these structures have a certain width, they are described by poles in the complex plane with a real part (the energy of the excitation) and a finite imaginary part (whose inverse is proportional to the excitation lifetime).

Since response functions represent the causal response of the system to external perturbations, they must obey several analytic properties and sum rules. The response function  $\chi_{\text{OP}}(\omega)$ , continued in the complex plane is analytic for all  $\Im\{\omega\} > 0$  in the upper half-plane and has poles only in the lower half-plane. Using contour integration in the complex plane, it is possible to obtain the Kramers-Kronig relations (Kramers 1927; Kronig 1926) that link the real and imaginary parts of  $\chi_{\text{OP}}$ :

$$\Re e \chi_{\text{OP}}(\omega) = -\frac{1}{\pi} \int_{-\infty}^{+\infty} d\omega' \frac{\Im m \chi_{\text{OP}}(\omega')}{\omega' - \omega}, \quad (3.35a)$$

$$\Im m \chi_{\text{OP}}(\omega) = -\frac{1}{\pi} \int_{-\infty}^{+\infty} d\omega' \frac{\Re e \chi_{\text{OP}}(\omega')}{\omega' - \omega}. \quad (3.35b)$$

The density-density response function  $\chi$  of Eq. 3.22 is an example of the more general response function of Eq. 3.31. It can be written in the Lehmann representation

$$\chi(\mathbf{r}, \mathbf{r}', \omega) = \sum_j \left[ \frac{\rho_j(\mathbf{r}) \rho_j^*(\mathbf{r}')}{\omega - E_j + E_0 + i\eta} - \frac{\rho_j^*(\mathbf{r}) \rho_j(\mathbf{r}')}{\omega + E_j - E_0 + i\eta} \right], \quad (3.36)$$



and it obeys the Kramers–Kronig relations Eq. 3.35. It is easy to see that the imaginary part of  $\chi$  has the form of a joint density of states weighted by matrix elements.

When we are interested in small perturbations induced by electromagnetic fields, which can be represented by a scalar potential  $v_{\text{ext}}$  and a vector potential  $\mathbf{A}_{\text{ext}}$ , besides defining density-density response functions, one has also to define density-current, current-density and current-current response functions. We will see in the next section that the macroscopic response of the system to a longitudinal (and within some limitations also to a transverse) perturbation can be recast in terms of the density-density response function  $\chi$  alone.

Now that we have understood how to provide a microscopic description of the (linear) response of the electronic system under perturbation, we are ready to discuss how averaging procedures allow to extract the desired macroscopic physical quantities.

### 3.6 Microscopic–Macroscopic Connection

For periodic systems, the most natural way to deal with spatial periodicity is to apply a Fourier transform:

$$\begin{aligned}\chi_{GG'}(\mathbf{q}, \omega) &= \chi(\mathbf{q} + \mathbf{G}, \mathbf{q} + \mathbf{G}', \omega) \\ &= \int d^3r \int d^3r' e^{-i(\mathbf{q} + \mathbf{G}) \cdot \mathbf{r}} \chi(\mathbf{r}, \mathbf{r}', \omega) e^{i(\mathbf{q} + \mathbf{G}') \cdot \mathbf{r}'},\end{aligned}\quad (3.37)$$

where  $\mathbf{G}$  is a vector of the reciprocal lattice, while  $\mathbf{q}$  is a vector in the first Brillouin zone. Therefore, we rewrite the microscopic response function (3.25) in the reciprocal space

$$\epsilon_{GG'}^{-1}(\mathbf{q}, \omega) = \delta_{GG'} + v_{\text{ee}}(\mathbf{q}) \chi_{GG'}(\mathbf{q}, \omega). \quad (3.38)$$

We are now in principle able to calculate a microscopic dielectric function. However, what is measured in an experiment is usually a macroscopic quantity, which involves averaging over regions of space that are large in comparison with the interparticle separation, but small compared to the wavelength of the perturbation. Special care is then necessary to bridge the gap between the microscopic and the macroscopic worlds in the case of extended systems.

Moreover, we should not forget that we are dealing with different dielectric functions, that are specific for transverse and longitudinal perturbations. For a non-vanishing  $\mathbf{q}$  and a non-cubic symmetry:

$$\mathbf{D}(\mathbf{q}, \omega) = \overleftrightarrow{\epsilon}_{\text{M}}(\mathbf{q}, \omega) \mathbf{E}^{\text{tot}}(\mathbf{q}, \omega), \quad (3.39)$$

where

$$\mathbf{D} = \begin{pmatrix} D^{\text{L}} \\ D^{\text{T}} \end{pmatrix} = \begin{pmatrix} \epsilon_{\text{M}}^{\text{LL}} & \epsilon_{\text{M}}^{\text{LT}} \\ \epsilon_{\text{M}}^{\text{TL}} & \epsilon_{\text{M}}^{\text{TT}} \end{pmatrix} \begin{pmatrix} E^{\text{L}} \\ E^{\text{T}} \end{pmatrix}.$$

This means that in general, a purely longitudinal or purely transverse perturbation will induce a longitudinal and a transverse response at the same time. Besides, transverse and longitudinal components of the dielectric tensor are no more equal, and only  $\epsilon_M^{\text{LL}}(\mathbf{q}, \omega)$  can be easily calculated, as we will show below, while  $\epsilon_M^{\text{TT}}(\mathbf{q}, \omega)$  obeys a complicated expression (Del Sole 1984). Only the high symmetry of the system can guarantee that a longitudinal (transverse) perturbation induces only a longitudinal (transverse) response. This happens when off-diagonal elements of (3.6) are zero. When the symmetry is lower, but still one is interested in the response in the long-wavelength limit, it is always possible to use the fact that the components of the dielectric tensor are analytic functions of  $\mathbf{q}$  in the limit  $\mathbf{q} \rightarrow 0$  and rewrite the tensor along the principal axes of the crystal. Applying a longitudinal perturbation along one of the principal axis induces only a longitudinal response. Of course, in the long-wavelength limit this same expression gives also the transverse dielectric function.

One can conclude that for perturbations with vanishing momentum transfer, the longitudinal and transverse responses (measured respectively in EELS and absorption experiments) coincide (see Eq. 3.20). There is no easy way to calculate the transverse response if it does not coincide with the longitudinal one. In that case, the general expression involves not only the density–density response function, but also current–current response functions. In view of the above, we consider here only the simpler longitudinal case. For a more general discussion the reader can refer to the work of Del Sole and Fiorino (1984) and the review of Strinati (1988).

In order to compare with optical and EELS spectra, we want to determine the longitudinal component of the macroscopic dielectric tensor (or possibly the three components along the principal axis). The (longitudinal) microscopic dielectric function can be obtained by the density–density response function  $\chi$  by applying Eq. 3.38. When the system is perturbed by an external scalar potential  $v_{\text{ext}}$ , the total potential (sum of the external and the induced potential) felt by a test-charge is:

$$v_{\text{tot}}(\mathbf{q} + \mathbf{G}, \omega) = \sum_{\mathbf{G}'} \epsilon_{\mathbf{G}, \mathbf{G}'}^{-1}(\mathbf{q}, \omega) v_{\text{ext}}(\mathbf{q} + \mathbf{G}', \omega). \quad (3.40)$$

The total potential in general has different wavevector components than the perturbing potential for the presence of microscopic fluctuations induced by the inhomogeneities of the material. The difference between the microscopic potentials and their macroscopic average are the already mentioned local-field effects.

To connect the microscopic and the macroscopic quantities one has to take a spatial average over a distance that is large compared to the lattice parameters and small compared to the wavelength of the external perturbation (Ehrenreich 1966). Since the microscopic quantities are lattice periodic, this procedure is equivalent to take the spatial average over a unit cell.

A microscopic potential  $v(\mathbf{r}, \omega)$  can be expanded in its Fourier components as:

$$v(\mathbf{r}, \omega) = \sum_{\mathbf{qG}} v(\mathbf{q} + \mathbf{G}, \omega) e^{i(\mathbf{q} + \mathbf{G}) \cdot \mathbf{r}}, \quad (3.41)$$

or:

$$v(\mathbf{r}, \omega) = \sum_{\mathbf{q}} e^{i\mathbf{q}\cdot\mathbf{r}} \sum_{\mathbf{G}} v(\mathbf{q} + \mathbf{G}, \omega) e^{i\mathbf{G}\cdot\mathbf{r}} = \sum_{\mathbf{q}} e^{i\mathbf{q}\cdot\mathbf{r}} v(\mathbf{q}, \mathbf{r}, \omega), \quad (3.42)$$

where:

$$v(\mathbf{q}, \mathbf{r}, \omega) = \sum_{\mathbf{G}} v(\mathbf{q} + \mathbf{G}, \omega) e^{i\mathbf{G}\cdot\mathbf{r}}. \quad (3.43)$$

$v(\mathbf{q}, \mathbf{r}, \omega)$  is periodic with respect to the Bravais lattice and hence is the quantity that one has to average to get the corresponding macroscopic potential  $v_M(\mathbf{q}, \omega)$ :

$$v_M(\mathbf{q}, \omega) = \frac{1}{\mathcal{V}} \int d\mathbf{r} v(\mathbf{q}, \mathbf{r}, \omega). \quad (3.44)$$

Inserting (3.43) in (3.44), one has:

$$v_M(\mathbf{q}, \omega) = \sum_{\mathbf{G}} v(\mathbf{q} + \mathbf{G}, \omega) \frac{1}{\mathcal{V}} \int d^3r e^{i\mathbf{G}\cdot\mathbf{r}} = v(\mathbf{q} + 0, \omega). \quad (3.45)$$

Therefore the macroscopic averaged potential  $v_M$  is given by  $\mathbf{G} = 0$  component of the corresponding microscopic potential  $v$ .

In particular, in the standard spectroscopy experiments discussed in this chapter, the external perturbing potential is a macroscopic quantity. For instance it can be the electromagnetic field impinging on a sample that one can measure in an absorption experiment. For Eq. 3.45 only the  $\mathbf{G} = 0$  component of  $v_{\text{ext}}(\mathbf{q} + \mathbf{G}, \omega)$  is different from 0. Therefore the macroscopic average  $v_{\text{tot},M}$  of the microscopic total potential  $v_{\text{tot}}$  in Eq. 3.40 is:

$$v_{\text{tot},M}(\mathbf{q}, \omega) = \epsilon_{\mathbf{G}=0, \mathbf{G}'=0}^{-1}(\mathbf{q}, \omega) v_{\text{ext}}(\mathbf{q}, \omega). \quad (3.46)$$

Equation 3.46 is a relation between macroscopic potentials, so it defines the macroscopic inverse dielectric function  $\epsilon_M^{-1}$ :  $v_{\text{tot},M} = \epsilon_M^{-1} v_{\text{ext}}$ . In this way one obtains:

$$\epsilon_M^{-1}(\mathbf{q}, \omega) = \epsilon_{\mathbf{G}=0, \mathbf{G}'=0}^{-1}(\mathbf{q}, \omega). \quad (3.47)$$

Therefore, the macroscopic dielectric function turns out to be defined as:

$$\epsilon_M(\mathbf{q}, \omega) = \frac{1}{\epsilon_{\mathbf{G}=0, \mathbf{G}'=0}^{-1}(\mathbf{q}, \omega)}. \quad (3.48)$$

This corresponds to the result found by Adler (1962) and Wiser (1963): the macroscopic dielectric function  $\epsilon_M$  is the reciprocal of the head (i.e. the  $\mathbf{G} = 0, \mathbf{G}' = 0$  element) of the inverse of the microscopic dielectric function  $\epsilon^{-1}$ .

It is important to note here that, since  $v_{\text{tot}}$  is in general a microscopic quantity, because it contains the microscopic fluctuations due to the polarization of the medium, one could not obtain directly the macroscopic dielectric function  $\epsilon_{\text{M}}$  from the inverse of the relation (3.40):

$$v_{\text{ext}}(\mathbf{q} + \mathbf{G}, \omega) = \sum_{\mathbf{G}'} \epsilon_{\mathbf{G}, \mathbf{G}'}(\mathbf{q}, \omega) v_{\text{tot}}(\mathbf{q} + \mathbf{G}', \omega). \quad (3.49)$$

Since  $v_{\text{ext}}$  is macroscopic, (3.49) is just:

$$v_{\text{ext}}(\mathbf{q}, \omega) = \sum_{\mathbf{G}'} \epsilon_{\mathbf{G}=0, \mathbf{G}'}(\mathbf{q}, \omega) v_{\text{tot}}(\mathbf{q} + \mathbf{G}', \omega). \quad (3.50)$$

Hence:

$$v_{\text{ext}}(\mathbf{q}, \omega) = \epsilon_{\mathbf{G}=0, \mathbf{G}'=0}(\mathbf{q}, \omega) v_{\text{tot}, \text{M}}(\mathbf{q}, \omega) + \sum_{\mathbf{G}' \neq 0} \epsilon_{\mathbf{G}=0, \mathbf{G}'}(\mathbf{q}, \omega) v_{\text{tot}}(\mathbf{q} + \mathbf{G}', \omega). \quad (3.51)$$

Since  $v_{\text{ext}} = \epsilon_{\text{M}} v_{\text{tot}, \text{M}}$ , one has that  $\epsilon_{\text{M}} = \epsilon_{\mathbf{G}=0, \mathbf{G}'=0}$  only if the off-diagonal terms ( $\mathbf{G}' \neq 0$ ) are neglected in Eq. 3.51. These off-diagonal terms correspond to the rapidly oscillating contributions to the microscopic total potential and are responsible for the crystal local-field effects. In fact, from Eq. 3.48, one has that  $\epsilon_{\text{M}} = 1/\epsilon_{\mathbf{G}=0, \mathbf{G}'=0}^{-1} = \epsilon_{\mathbf{G}=0, \mathbf{G}'=0}$  only if  $\epsilon_{\mathbf{G}, \mathbf{G}'}$  is diagonal, which corresponds to a dielectric function in the real space that depends only on the distance between  $\mathbf{r}$  and  $\mathbf{r}'$ .

It is possible to prove (Hanke 1978; Onida 2002) that  $\epsilon_{\text{M}}$  can be directly obtained using a modified density–density response function  $\bar{\chi}$  :

$$\epsilon_{\text{M}}(\mathbf{q}, \omega) = 1 - v_{\text{ee}} \mathbf{G}=0(\mathbf{q}) \bar{\chi}_{\mathbf{G}=0, \mathbf{G}'=0}(\mathbf{q}, \omega). \quad (3.52)$$

Whereas the density-density response function  $\chi$  satisfies the Dyson equation (1.3.eq:chi-P)  $\chi = P + P v_{\text{ee}} \chi$ , the modified response function  $\bar{\chi}$  is obtained from

$$\bar{\chi} = P + P \bar{v}_{\text{ee}} \bar{\chi}, \quad (3.53)$$

where the macroscopic component of  $\bar{v}_{\text{ee}}$  is set to zero:  $\bar{v}_{\text{ee} \mathbf{G}=0} = 0$  and for all the other components it holds  $\bar{v}_{\text{ee}} = v_{\text{ee}}$ . Neglecting local-field effects (NLF), the macroscopic dielectric function is (see Eq. 3.51):

$$\epsilon_{\text{M}}^{\text{NLF}}(\mathbf{q}, \omega) = \epsilon_{\mathbf{G}=0, \mathbf{G}'=0}(\mathbf{q}, \omega) = 1 - v_{\text{ee} \mathbf{G}=0}(\mathbf{q}) P_{\mathbf{G}=0, \mathbf{G}'=0}(\mathbf{q}, \omega). \quad (3.54)$$

Therefore, comparing (3.52) and (3.54), one can see that it is the microscopic part of the Coulomb interaction  $\bar{v}$  that is responsible for the local-field effects. In fact, setting  $\bar{v} = 0$  in (3.53) would imply that  $\bar{\chi} = P$  and hence  $\epsilon_{\text{M}}^{\text{NLF}} = \epsilon_{\text{M}}$ .

Local-field effects are tightly related to spatial inhomogeneities in the system. Whenever a system is inhomogeneous, even if the external field is slowly varying,

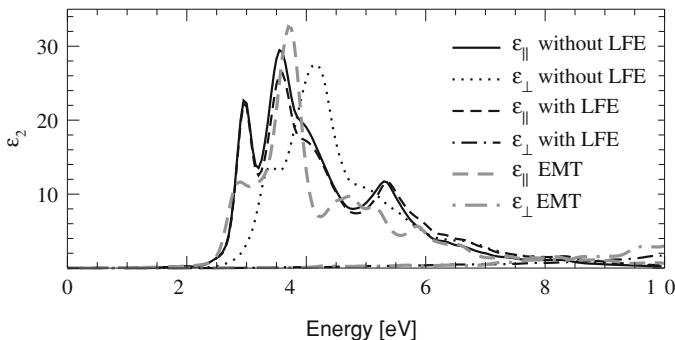


**Fig. 3.4** Imaginary part of the dielectric function for a [110] Si nanowire, with a diameter of 2.2 nm. Calculations are performed for light polarized along ( $\epsilon_{\parallel}$ ) and perpendicularly ( $\epsilon_{\perp}$ ) to the wire axis, starting from a DFT-LDA ground state and using the RPA approximation either including local-field effects (with LFE) or neglecting them (without LFE). The result of a classical effective medium theory (Maxwell-Garnett 1904) (which accounts for classical local-field effects) is shown for comparison (*grey lines*). Figure from Bruneval (2005)

the induced charges can have rapid spatial variations. This means that the off-diagonal elements of the dielectric function are important. Typical examples where local fields play an important role (Botti 2007) are layered systems, nanotubes or nanowires, and finite systems like nanoclusters, which represent themselves an inhomogeneity in the vacuum space. Instead, bulk solids of *sp* semiconductors are often examples of homogeneous systems where local fields play a minor role. In Fig. 3.4 (Bruneval 2005) we show the optical absorption of a Si nanowire with a diameter of 2.2 nm, calculated including and neglecting local-field effects. By neglecting local-field effects one obtains a similar optical absorption for the two components of the imaginary part of the dielectric functions along and perpendicular to the wire axis (solid and dotted lines). When local-field effects are included, no significant changes in the parallel component (dashed line) are observed. In fact, the inhomogeneity of the nanowire is pronounced in the direction perpendicular to the wire axis, which explains why it turns out that  $\epsilon_{\perp}$  (dash-dotted line) is extremely sensitive to the local-field effects: the absorption is shifted to higher energies and the nanowire becomes transparent up to 6–7 eV. This result can be better understood if we use the fact that, for large wires, the *ab initio* calculations tend to reproduce the classical limit given by the effective-medium theory (Maxwell-Garnett 1904), that accounts for the classical effects due to the gathering of charges at the polarized surface of the wire.

These criteria to evaluate the importance of local-field effects actually apply only for polarizable systems, where the initial and final states involved in a particular transition are localized in a common spatial region (Aryasetiawan 1994). On the contrary, even in strongly inhomogeneous systems, if the inhomogeneity is not very polarizable, the induced potentials are small and consequently local fields are not so important.

Absorption and electron energy-loss experiments measure  $\Im m \{\epsilon_M\}$  and  $-\Im m \{\epsilon_M^{-1}\}$ , respectively. Once  $\epsilon_{G,G'}$  has been calculated, the spectra are obtained from:

$$\text{Abs}(\omega) = - \lim_{q \rightarrow 0} \Im m \{\epsilon_M(\omega)\} = - \lim_{q \rightarrow 0} \Im m \left\{ \frac{1}{\epsilon_{G=0,G'=0}^{-1}(\mathbf{q}, \omega)} \right\}, \quad (3.55a)$$

$$\text{EELS}(\omega) = - \lim_{q \rightarrow 0} \Im m \left\{ \epsilon_M^{-1}(\omega) \right\} = - \lim_{q \rightarrow 0} \Im m \left\{ \epsilon_{G=0,G'=0}^{-1}(\mathbf{q}, \omega) \right\}, \quad (3.55b)$$

where, in particular, we considered EELS at vanishing momentum transfer. Equivalently:

$$\text{Abs}(\omega) = - \lim_{q \rightarrow 0} \Im m \left\{ v_{ee G=0}(\mathbf{q}) \bar{\chi}_{G=0,G'=0}(\mathbf{q}, \omega) \right\}, \quad (3.56a)$$

$$\text{EELS}(\omega) = - \lim_{q \rightarrow 0} \Im m \left\{ v_{ee G=0}(\mathbf{q}) \chi_{G=0,G'=0}(\mathbf{q}, \omega) \right\}. \quad (3.56b)$$

The only difference between  $\bar{\chi}$  and  $\chi$  is the absence of the long-range term  $v_{ee G=0}$  of the Coulomb interaction in the Dyson equation (3.53). Therefore  $v_{ee G=0}$  is the responsible for the difference between absorption and EELS spectra in solids (Sottile 2005). Bulk silicon absorbs in the energy range between 3–5 eV and the plasmon resonance is at 16.8 eV. In finite systems, instead, the long-range term becomes negligible. For this reason, when the limit  $q \rightarrow 0$  is assumed, EELS and absorption mathematically coincide in finite systems.

### 3.7 Conclusions

In this chapter we have discussed how to model processes involving one-particle and neutral excitations, such as photoemission, inverse photoemission, optical absorption and electron energy loss spectroscopies, in order to calculate spectra directly comparable with experimental data.

We analyzed which physical approximations are involved in the microscopic modeling of the interaction of radiation (or particles) and matter, and how they affect the comparison with experimental spectra. When it is necessary to obtain macroscopic response functions from microscopic ones, a special care must be taken in performing appropriate averaging procedures.

Only in the simple case of a cubic system and a vanishing wavevector the dielectric function is a scalar quantity, otherwise we must consider a tensor that contains components related to the response of the system to a longitudinal and transverse perturbation. In the long-wavelength limit the longitudinal and transverse responses coincide, which is essential to calculate optical absorption, as a simple expression in terms of the density-density response function exists for the longitudinal component of the dielectric tensor.